Sciencexpress Reports

Living Crystals of Light-Activated Colloidal Surfers

Jeremie Palacci,[1]* Stefano Sacanna,[1] Asher Preska Steinberg,[2] David J. Pine,[1] Paul M. Chaikin[1]

[1]Department of Physics, New York University, 4 Washington Pl., New York, NY 10003, USA. [2]Department of Physics and Chemistry, Brandeis University, Waltham, MA 02453, USA.

*To whom correspondence should be addressed. E-mail: Jeremie Palacci: jp153@nyu.edu

Spontaneous formation of colonies of bacteria or flocks of birds are example of self-organization in active living matter. Here we demonstrate a form of self-organization from nonequilibrium driving forces in a suspension of synthetic photoactivated colloidal particles. They lead to two dimensional "living crystals" which form, break, explode and reform elsewhere. The dynamic assembly results from a competition between self-propulsion of particles and an attractive interaction induced respectively by osmotic and phoretic effects and activated by light. We measure a transition from normal to giant number fluctuations. Our experiments are quantitavely described by simple numerical simulations. We show that the existence of the living crystals is intrinsically related to the out-of-equilibrium collisions of the self-propelled particles.

Self-organization often develops in thermal equilibrium as a consequence of entropy and potential interactions. However, there are a growing number of phenomena where order arises in driven, dissipative systems, far from equilibrium. Examples include "random organization" of sheared colloidal suspensions (*1*) and rods (*2*), nematic order from giant number fluctuations in vibrated rods (*3*) and phase separation from self-induced diffusion gradients (*4*). Biological (*5–7*) and artificial active particles (*8–11*), also exhibit swarm patterns that result from their interactions (*12–15*).

In order to study active, driven, collective phenomena we created a system of self-propelled particles where the propulsion can be turned on and off with a blue light. This switch provides rapid control of particle propulsion and a convenient means to distinguish non-equilibrium activity from thermal Brownian motion. Further, the particles are slightly magnetic and can be stabilized and steered by application of a modest magnetic field. Our system consists of an active bimaterial colloid. A polymer sphere, 3-methacryloxypropyl trimethoxysilane (TPM), encapsulates most of a canted anti-ferromagnetic hematite cube (*16*), but with part exposed to the solvent, as show in Fig. 1A. The particles are immersed in a basic solution (pH ~ 8.5) containing hydrogen peroxide (0.1 to 3% w/w), 5 mM tetramethylammonium hydroxide and 3.4 mM sodium dodecyl sulfate (*16*). Under normal bright field illumination, the colloids are at equilibrium with the solvent and thus sediment toward the bottom glass surface of the observation cell. When illuminated through the microscope objective with blue-violet light ($\lambda \sim 430{-}490$nm), the particles exhibit self-propulsion (see movie S1). The motion, with a velocity up to 15 μm/s, only takes place at the cell surface, whether it is the bottom, the vertical side walls or the cell top. Individual particles undergo a random walk with a persistence length determined by the reorientation time τ_r=8.0 ± 1.5 s consistent with Stokes-Einstein rotational diffusion.

In equilibrium, with no blue light, the particles diffuse and are disordered, as shown in the inset of Fig. 1B. At surface area fractions Φ_s >~7% cooperative behavior of the light-activated colloids begins to emerge. Crystallites start to form in the sample 25 s after the light is turned on. An image of the crystals after 350s is shown in the main panel in Fig. 1B. Immediately after the light is extinguished, the crystallites begin "dissolving" due to thermal diffusion (Fig. 1C); after 100s there is no trace of the crystals (Fig. 1C insert). While the particles form organized crystallite structures under illumination, those structures are not static (see movie S2). As shown in Fig. 1D-G, the crystallites actively translate and rotate, collide, join, and split, as shown in Fig. 1D-G. These "living crystals" reach a dynamic steady state of creation and self-destruction. They do not grow to incorporate all available particles as would be the case for an equilibrium system with attractive interactions. We measure an average cluster size of ~ 35 particles which does not seem to depend on the surface coverage fraction, Φ_s > 10%. The lifetime of the crystals is finite and broadly distributed. The typical time for a cluster to change its size by 50% is 100 ± 75s. Fluctuations in the local number N of particles follows a power law $\Delta N \sim N^{\alpha}$. There is a transition at $\Phi_S \sim 7\%$ from normal $\alpha = [1/2]$ to giant fluctuations $\alpha \cong 0.9$, in line with recent predictions for disordered clusters in a system of polar isotropic active particles (*17*) and observed in a granular system (*18*).

To understand the mechanisms involved in the self-propulsion and crystallization we performed a series of experiments on the separate components of our composite colloid, the hematite cube and the polymer sphere. First, we attach a hematite cube to a glass substrate and immerse it in our solution of surfactants, buffer, and H_2O_2. 1.5 μm diameter colloidal tracer particles of polystyrene, silica, or TPM, are added. The tracers are observed to diffuse randomly under normal bright field illumination. When illuminated with blue light, however, the tracers all move toward the immobilized hematite cube (see movie S3), converging on it from all directions, as indicated by the cartoon in Fig. 2A. This observation rules out advection, as advective fluid flow must have zero divergence. Therefore, the motion of the colloids toward the hematite particle must be caused by a phoretic motion (*19*) induced by some gradient generated by the cube. Under blue light illumination, hematite catalyses the exothermic chemical decomposition of H_2O_2 creating thermal and chemical (H_2O_2 and O_2) gradients. Heating studies of the system suggest that diffusiophoresis is more important than thermophoresis in our system. The motion of the tracers toward the cube can be quantified by monitoring their position versus time and calculating their velocity as a function of distance from the particle (Fig. 2B). The dashed line through the data is a fit to A/r^2 consistent with a diffusive concentration profile $C \propto C_{\infty}(1{-}B/r)$.

Phoresis and osmosis are complementary interfacial phenomena: in a gradient, a free colloid will exhibit a phoretic migration while a fixed surface of the same material will exhibit an osmotic flow at its surface in the opposite direction (*19*). Therefore a particle phoresing to the right has an osmotic flow at its surface to the left. Just as a silica colloid is attracted to a hematite cube, a free hematite particle is attracted to a stationary silica surface. Therefore, when we add free cubes to a sample cell, the silica surface of the cover slip attracts the cubes. Indeed, we observe that hematite cubes are quickly drawn to the glass substrate as soon as blue light is turned on.

Surprisingly, once on the glass substrate, the hematite cubes continue to move on the glass surface when illuminated with blue light. Naïvely, one might expect the cubes to remain stationary, as the osmotic flow

on the cover slip surface is away from the cube and ideally should be symmetric. However, the symmetry is broken either by imperfections on the cube or spontaneously by an instability where the motion of the cube induces different gradients fore and aft. Thus, in a solution of free hematite cubes we see attraction of the cubes to the surface followed by self propulsion of the cubes surfing on the substrate when the light is turned on.

When using a suspension of our composite particles, a hematite cube in a TPM sphere, we observe a similar scenario. When illuminated with blue light, the composite particle reorients so that the exposed hematite sits on the glass substrate, as shown in Fig. 2C (insets), and then begins to move at speeds comparable to the hematite alone. Figure 2C shows the trajectory of a single composite particle, with the light turned on then off, while the insert shows a superposition of many trajectories with their origins aligned. The self-propelled motions are isotropic and diffusive with a persistence length (15−100 μm) determined by the rotational diffusion time and the velocity of the particle. The velocity of the particles depends weakly on the H_2O_2 concentration but strongly on the light intensity and the Debye screening length. In Fig. 2D we see that the velocity versus light intensity P follows Michaelis-Menten law (*20*) behavior characteristic of a catalytic reaction. Figure 2E suggests that the composite particle velocity asymptotes to a quadratic behavior with Debye length λ_D (*21*), a behavior expected from osmotic effects within a Debye length of a surface where the driving force $\propto \lambda_D$ and the drag force is $\propto$ velocity/λ_D (*19*, *22*).

If we now consider a solution of composite particles activated by light, two effects have to be taken into account *(i)* the collisions between our self-propelled particles surfing on the osmotic flow they set-up and *(ii)* the phoretic attraction between the particles. In order to see if these effects explain the formation of our living crystals, we performed simulations guided by our experimentally determined parameters.

We consider a minimal numerical model (*16*) in which the self-propelled colloids are represented by self-propelled hard disks that move with a constant velocity in a direction that changes randomly on a time scale τ_r determined by rotational diffusion. We model the phoretic attraction between particles as a pairwise attraction between nearby particles consistent with the phoretic velocity shown as the red line in Fig. 2B. If a displacement makes two disks overlap, the particles are separated by moving each one half the overlap distance along their center-to-center axis. We have tried various approximations to account for the effect of (hydrodynamic) lubrication forces in the crystals, *e.g.* increase of the apparent viscosity, and find little qualitative difference.

In Fig. 3 and movie S4, we present the results of simulations in which the attractive phoretic effects are taken into account. For our experimental conditions $\Phi_s \sim 3-20\%$ and $\sim 300-1500$, the simulations reproduce the crystallite formation as well as the size and lifetime of the crystallites remarkably well. As shown on Fig. 4.A, B the simulations also capture the transition observed experimentally from normal to giant fluctuations of number, above a critical density $\Phi^C_S \cong 7\%\pm1\%$. If we turn off the pairwise phoretic attraction, we observe large spatio-temporal fluctuations of density with normal number fluctuations, $\alpha \sim 0.5$ (see Fig. 4.B). The formation of clusters which grow and decay is recovered at much higher particle concentration, $\Phi_s >\sim 35-45\%$ (see Fig. S2).

Our understanding of the living crystals comes from the idea that active particles undergo diffusive motion with a large persistence length when not in "contact" but slow down, translate and diffuse more slowly, when they are in contact. The slowing down results from the inability of particles to penetrate their neighbors when encountered.

Several recent papers have pointed out that such density dependent diffusion can lead to giant fluctuations, clustering and phase separation in non-equilibrium systems (*17*, *23–26*), however at much larger surface density. The formation of non-crystalline clusters of active particles has been reported with bacteria coupled through short-range depletion interaction (*27*) and Janus particles with chemical attraction (*28*).

We always observe the intermittent formation and breakage of the large crystals. This differs from the equilibrium nucleation and growth of a crystal of attractive colloids or the asymptotic formation of a single cluster from an assembly of self-propelled disks reported by Fily and Marchetti (*17*) (however at higher number and density of disks than in our experiment).

In order to investigate the underlying mechanisms, we take advantage of the magnetic properties of the embedded hematite cube. Under an external magnetic field ($B \sim 1$ mT), the alignment of the hematite slighty tilts the orientation of the particle and the self-propulsion proceeds in a direction parallel to the field, suppressing the rotational diffusion.

We test two crucial aspects of our scenario in Fig. 4D-I and Movie S5. We suggest that the crystal breakup depends on the velocity redirection by rotational diffusion of the particles in the crystal. If the direction of all the particles are aligned using an external magnetic field then the crystal will not break up. This is shown in Fig. 4. D-E, Movie S5. Also note the suppression of the breakup in the magnetically steered crystal in Movie S6. We also claim that collisions are required for crystal formation. In Fig. 4F we turn off the light and the crystal dissolves. With the magnetic field off, we turn on the light, the particles collide and the crystal reforms, Fig. 4G. We turn off the light and redissolve the crystal in Fig. 4H. We then first turn on the magnetic field and then the light., in Fig. 4I. The particles all move in the same direction, do not collide and there is no crystallization.

We have demonstrated a new form of self-assembly from non-equilibrium driving forces leading to "living crystals" with complex dynamics. The osmotically driven motion and steric hindrances lead to the formation of dynamic aggregates. The introduction of a small attractive interaction, in this case arising from phoresis, orders the aggregates into periodic crystals at low surface fraction. Phoretic and osmotic effects in our system can conveniently be switched on and off by light. Rotational diffusion of the particles reorients their motions, leading to a finite persistence length, crystal evaporation and breakup and finite size and lifetime of the crystals. The use of active particles and nonequilibrium forces for directed self-assembly opens a new area for design and production of novel and moving structures. The fact that they can be turned on and off with visible light adds control to this system as does the ability to use external magnetic steering.

References and Notes

1. L. Corte, P. M. Chaikin, J. P. Gollub, D. J. Pine, Random organization in periodically driven systems. *Nat. Phys.* **4**, 420 (2008). doi:10.1038/nphys891
2. A. Franceschini, E. Filippidi, E. Guazzelli, D. J. Pine, Transverse alignment of fibers in a periodically sheared suspension: an absorbing phase transition with a slowly varying control parameter. *Phys. Rev. Lett.* **107**, 250603 (2011). doi:10.1103/PhysRevLett.107.250603 Medline
3. V. Narayan, S. Ramaswamy, N. Menon, Long-lived giant number fluctuations in a swarming granular nematic. *Science* **317**, 105 (2007). doi:10.1126/science.1140414 Medline
4. M. E. Cates, D. Marenduzzo, I. Pagonabarraga, J. Tailleur, Arrested phase separation in reproducing bacteria creates a generic route to pattern formation. *Proc. Natl. Acad. Sci. U.S.A.* **107**, 11715 (2010). doi:10.1073/pnas.1001994107 Medline
5. J.-F. Joanny, S. Ramaswamy, Biological physics: Filaments band together. *Nature* **467**, 33 (2010). doi:10.1038/467033a Medline
6. A. Cavagna *et al*., Scale-free correlations in starling flocks. *Proc. Natl. Acad. Sci. U.S.A.* **107**, 11865 (2010). doi:10.1073/pnas.1005766107 Medline
7. M. Polin, I. Tuval, K. Drescher, J. P. Gollub, R. E. Goldstein, Chlamydomonas swims with two "gears" in a eukaryotic version of run-and-tumble locomotion. *Science* **325**, 487 (2009). doi:10.1126/science.1172667 Medline
8. R. Dreyfus *et al*., Microscopic artificial swimmers. *Nature* **437**, 862 (2005). doi:10.1038/nature04090 Medline

9. W. F. Paxton *et al*., Catalytic nanomotors: autonomous movement of striped nanorods. *J. Am. Chem. Soc.* **126**, 13424 (2004). doi:10.1021/ja047697z Medline
10. J. R. Howse *et al*., Self-motile colloidal particles: from directed propulsion to random walk. *Phys. Rev. Lett.* **99**, 048102 (2007). doi:10.1103/PhysRevLett.99.048102 Medline
11. J. Palacci, C. Cottin-Bizonne, C. Ybert, L. Bocquet, Sedimentation and effective temperature of active colloidal suspensions. *Phys. Rev. Lett.* **105**, 088304 (2010). doi:10.1103/PhysRevLett.105.088304 Medline
12. D. Saintillan, M. J. Shelley, Instabilities, pattern formation, and mixing in active suspensions. *Phys. Fluids* **20**, 123304 (2008). doi:10.1063/1.3041776
13. H. P. Zhang, A. Be'er, E. L. Florin, H. L. Swinney, Collective motion and density fluctuations in bacterial colonies. *Proc. Natl. Acad. Sci. U.S.A.* **107**, 13626 (2010). doi:10.1073/pnas.1001651107 Medline
14. T. Vicsek, A. Czirók, E. Ben-Jacob, I. Cohen, O. Shochet, Novel type of phase transition in a system of self-driven particles. *Phys. Rev. Lett.* **75**, 1226 (1995). doi:10.1103/PhysRevLett.75.1226 Medline
15. G. Grégoire, H. Chaté, Onset of collective and cohesive motion. *Phys. Rev. Lett.* **92**, 025702 (2004). doi:10.1103/PhysRevLett.92.025702 Medline
16. Materials and methods are available as supporting material on *Science* Online.
17. Y. Fily, M. C. Marchetti, Athermal phase separation of self-propelled particles with no alignment. *Phys. Rev. Lett.* **108**, 235702 (2012). doi:10.1103/PhysRevLett.108.235702 Medline
18. J. Deseigne, O. Dauchot, H. Chaté, Collective Motion of Vibrated Polar Disks. *Phys. Rev. Lett.* **105**, 9 (2010). doi:10.1103/PhysRevLett.105.098001
19. J. Anderson, Colloid Transport by Interfacial Forces. *Annu. Rev. Fluid Mech.* **21**, 61 (1989). doi:10.1146/annurev.fl.21.010189.000425
20. L. Michaelis, M. Menten, *Biochem. Z.* **49**, 333 (1913).
21. J. Israelachvili, Intermolecular and Surface Forces, Elsevier, (2011).
22. R. Golestanian, T. B. Liverpool, A. Ajdari, Propulsion of a molecular machine by asymmetric distribution of reaction products. *Phys. Rev. Lett.* **94**, 220801 (2005). doi:10.1103/PhysRevLett.94.220801 Medline
23. J. Bialké, T. Speck, H. Löwen, Crystallization in a dense suspension of self-propelled particles. *Phys. Rev. Lett.* **108**, 168301 (2012). doi:10.1103/PhysRevLett.108.168301 Medline
24. S. R. McCandlish, A. Baskaran, M. F. Hagan, Spontaneous segregation of self-propelled particles with different motilities. *Soft Matter* **8**, 2527 (2012). doi:10.1039/c2sm06960a
25. F. Farell, J. Tailleur, D. Marenduzzo, M. Marchetti, *Phys. Rev. Lett.* **108**, 2248101 (2012).
26. J. Tailleur, M. E. Cates, Statistical mechanics of interacting run-and-tumble bacteria. *Phys. Rev. Lett.* **100**, 218103 (2008). doi:10.1103/PhysRevLett.100.218103 Medline
27. J. Schwarz-Linek *et al*., Phase separation and rotor self-assembly in active particle suspensions. *Proc. Natl. Acad. Sci. U.S.A.* **109**, 4052 (2012). Medline
28. I. Theurkauff, C. Cottin-Bizonne, J. Palacci, C. Ybert, L. Bocquet, Dynamic clustering in active colloidal suspensions with chemical signaling. *Phys. Rev. Lett.* **108**, 268303 (2012). doi:10.1103/PhysRevLett.108.268303 Medline
29. T. Sugimoto, M. M. Khan, A. Muramatsu, Preparation of monodisperse peanut-type α-Fe2O3 particles from condensed ferric hydroxide gel. *Colloids and Surfaces A* **70**, 2 (1993). doi:10.1016/0927-7757(93)80285-M
30. J. C. Crocker, D. G. Grier, Methods of Digital Video Microscopy for Colloidal Studies. *J. Colloid Interface Sci.* **179**, 1 (1996). doi:10.1006/jcis.1996.0217

Acknowledgments: We thank J. Layné, K. Hanson, A. Grosberg, R. Dreyfus, E. Lerner, A. Baskaran, L. Bocquet for fruitful discussions. This work was supported by the MRSEC Program of the National Science Foundation under Award Number DMR-0820341 and by the U. S. Army Research Office under Grant Award No. W911NF-10-1-0518. We acknowledge partial support from the NASA under Grant Award NNX08AK04G.

Supplementary Materials
www.sciencemag.org/cgi/content/full/science.1230020/DC1
Materials and Methods
Figs. S1 and S2
References (*29*, *30*)
Movies S1 to S6

11 September 2012; accepted 12 December 2012

Published online 31 January 2013
10.1126/science.1230020

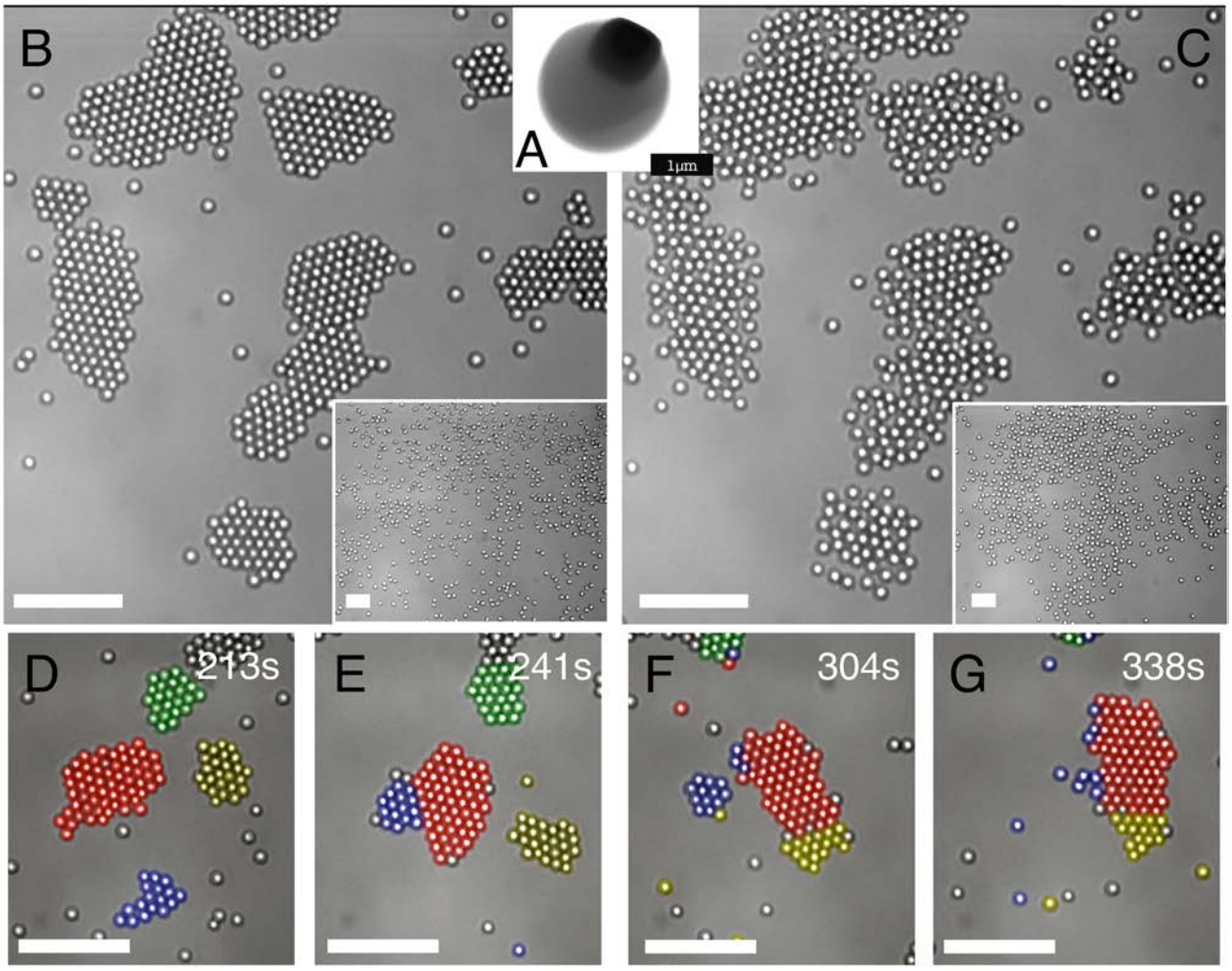

Fig. 1. (**A**) SEM of the bimaterial colloid: a TPM polymer colloidal sphere with protruding hematite cube (dark). (**B**) Living crystals assembled from a homogeneous distribution (inset) under illumination by blue light. (**C**) Living crystals melt by thermal diffusion when light is extinguished: image shows system 10 s after blue light is turned off (inset, after 100 s). (**D**-**G**). The false colors show the time evolution of particles belonging to different clusters. The clusters are not static but rearrange, exchange particles, merge (D→F), break apart (E→F) or become unstable and explode (blue cluster, F→G). For B-G, the scale bar is 10 μm. The solid area fraction is $\Phi_s \approx 0.14$.

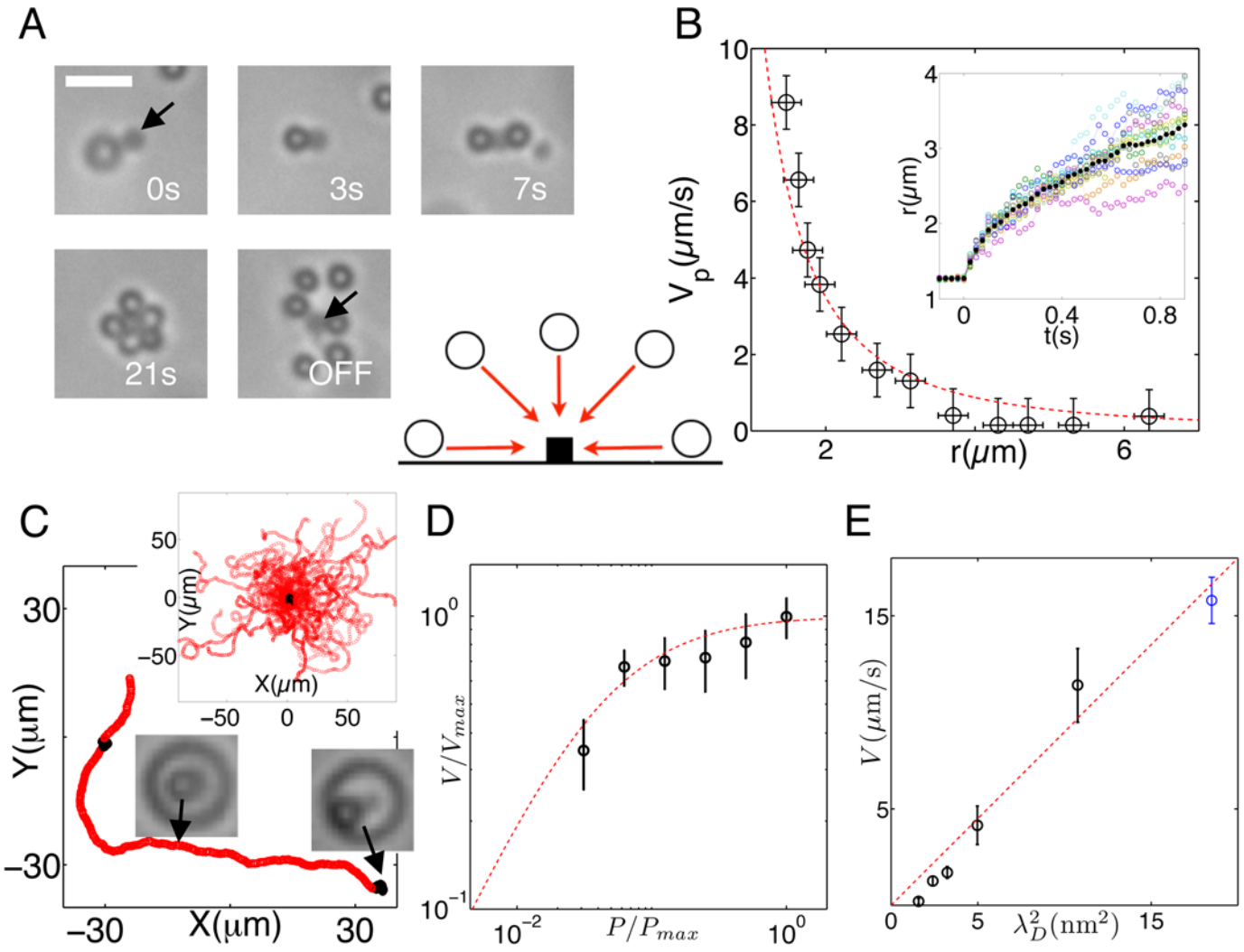

Fig. 2. Out-of-equilibrium driving forces. (**A**) A hematite cube, indicated by an arrow, is immobilized on a surface and immersed in a solution of colloidal tracers. At *t*=0 s, the blue light is switched on triggering the decomposition of hydrogen peroxide on the hematite surface. The tracers are attracted to the hematite until they contact the cube. The attraction is isotropic with particles coming from all directions, thus discounting advective flow which must exhibit zero divergence. When the light is turned off, the attraction ceases and the tracers diffuse away. (**B**) The attraction is quantified by the radial velocity V_p extracted from the ensemble average of the tracer drift (inset, black symbols) and is consistent with the r^{-2} behavior (red dashed line) expected for phoretic attraction to a reaction source. (**C**) A hematite cube protruding from a TPM polymer sphere moves on fixed glass substrate when exposed to blue light (red part of trace) and diffuses when the light is off (black part of trace). Initially, with no light, the hematite cube is oriented randomly (image, right), but rotates and faces downward toward the glass substrate when the light is turned on (image, left). The particle then surfs on the osmotic flow it induces between the substrate and itself. The inset shows a superposition of the trajectories of many particles with their origins aligned. (**D**) The particle velocity V increases with light intensity P and follows Michaelis-Menten law (red dashed line). The black arrow indicates the point of zero velocity for P=0. (**E**) The particle velocity is also strongly dependent on the Debye length λ_D of the system and asymptotically follows the $V \propto \lambda_D^2$ scaling expected for osmotic mechanisms (red dashed line). The Debye length is varied adding NaCl to the buffer solution except for the blue symbol for which the SDS surfactant is suppressed to reach higher λ_D. The error bars in (D) and (E) are given by the standard deviation of the velocity measured for 10 to 20 different particles.

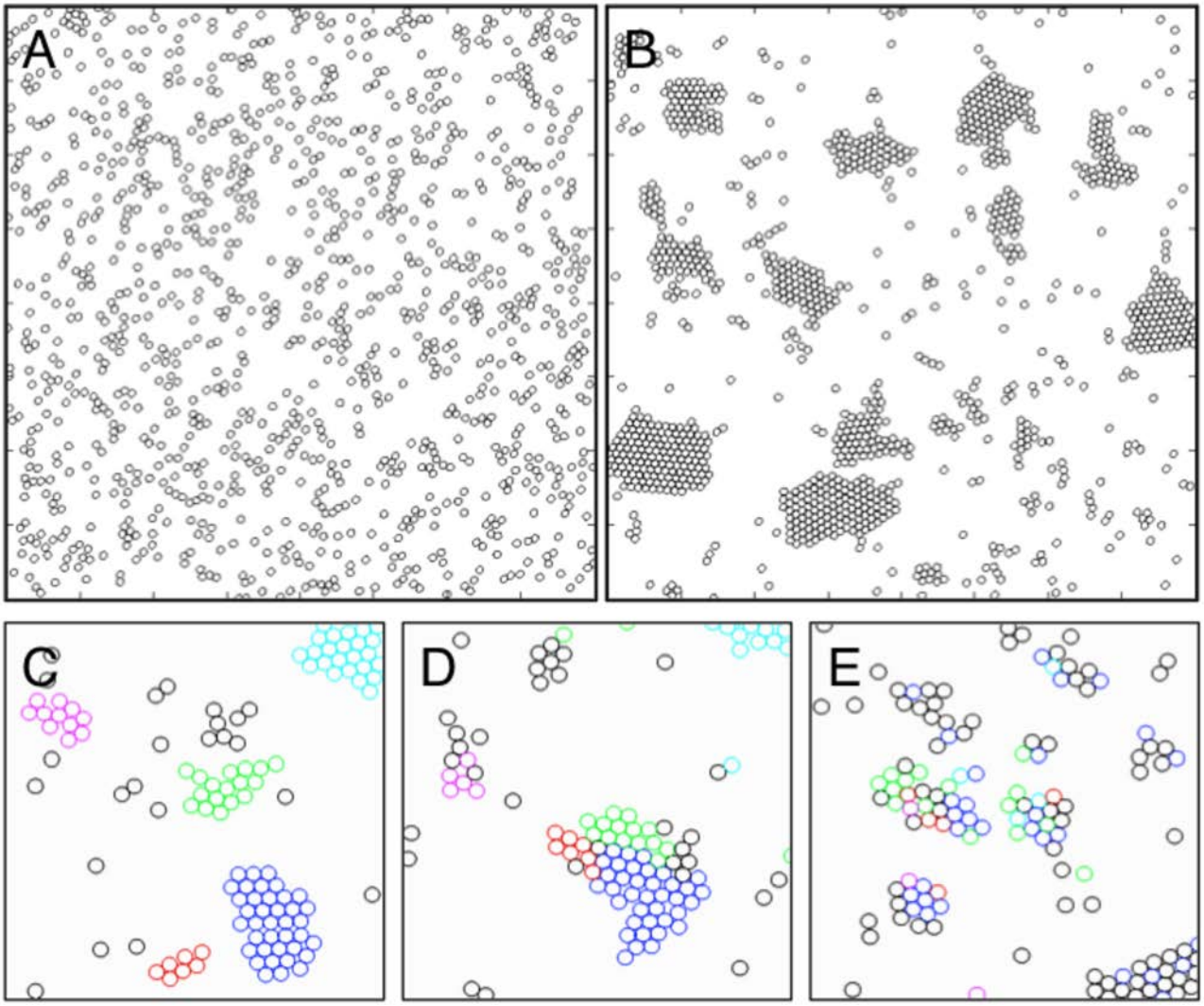

Fig. 3. Numerical simulations of self-propelled disks coupled by a phoretic attraction. Simulation parameters are defined to mimic the experimental conditions. (**A**) Starting from a homogeneous distribution, (**B**, $\sim t=8\sim\tau_r$) the disks assemble in mobile crystalline clusters with faceted edges. (**C**-**E**) The false colors show the time evolution of particles belonging to different clusters. The crystals are mobile (C, D, E), can merge (C, D), and break apart or dissolve (D, E). This minimal model reproduces the experimental dynamics of the "living crystals" and demonstrates the relevance of the proposed mechanism. We use parameters consistent with the experimental conditions of Fig. 1: Φ_s=0.14, $\sim\tau_r$=16 and $\sim A$=0.87 (see (*16*) for a definition of the reduced parameters, indicated by tildes).

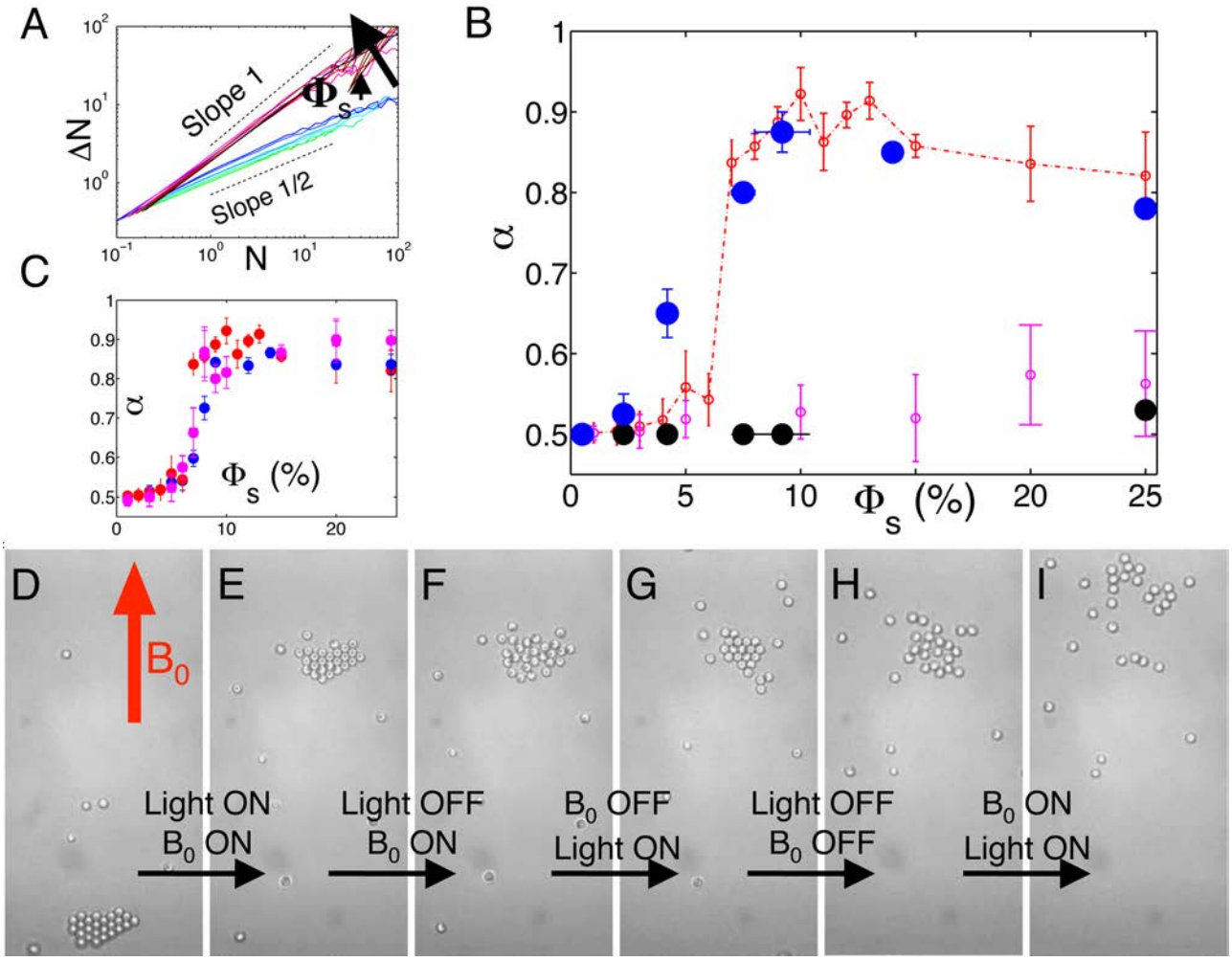

Fig. 4. (**A**) Number fluctuations measured in the simulations for varying surface fraction Φ_s, in the range 1−15% for N=600 particles (~τ_r=16 and ~A=0.87 from the experiment, see (*16*)). The system exhibits a transition from normal to giant fluctuations for $\Phi_s^C \sim 7\%$. (**B**) Scaling α of the number fluctuations, $\Delta N \propto N^{\alpha}$, for various surface coverage Φ_s measured in the experiment at equilibrium (black symbols), under activation by the light (blue symbols) and in the simulations with (~A=0.87, red empty symbols) and without attraction (~A=0, magenta empty symbols). We observe normal fluctuations, α = 1/2, at equilibrium. The driven system exhibits a transition from normal fluctuations, α = 1/2, to giant number fluctuations, α ~ 0.9, at $\Phi_s \sim 7\%$ in both the experiment and the simulations. The slight decay of the exponent observed in experiments and simulations is a finite size effect. (**C**) Scaling α of the number fluctuations for N=1000 (blue symbols), N=600 (red) and N=400 (magenta) particles in the simulations. For N=400, the curve after $50\tau_p$ (square) collapses with $35\tau_p$ (circles) showing that the scaling is steady. (**D-I**) Investigating the crystal mechanism. We use an external magnetic field $B_0 \sim 1$mT to orient the particles and direct their motion. The red arrow is the orientation of B_0. (**D, E**) The magnetic field is turned on and the light is on, the crystal is self-propelled in the direction of the magnetic field, crystal breakup is suppressed. (**F**) The light is turned off and the magnetic field B_0 is left, the crystal dissolves. (**G**) The magnetic field is turned off and the light is turned on, particles collide and the crystal reforms. (**H**) The light is turned off and the magnetic field remains off, the crystal dissolves. (**I**) The magnetic field is turned on first and then the light is turned on, the particles all move in the the field direction, they do not collide and do not crystallize.